

## Study on flax fiber toughened poly (lactic acid) composites

Xuelian Xia, Wentao Liu, Liyong Zhou, Hao Liu, Suqin He, Chengshen Zhu

School of Materials Science and Engineering, Zhengzhou University, Zhengzhou 450052, China

Correspondence to: W. Liu (E-mail: wtliau@zzu.edu.cn)

**ABSTRACT:** Poly (lactic acid) (PLA) is a renewable and biodegradable polymer with high modulus, high strength but low toughness. Blending PLA with plant fiber has been believed an available strategy to improve the toughness of PLA. PLA/Flax composites were fabricated by extrusion and injection molding processes. The flax fiber surfaces were modified before blending to improve the compatibility, and the chemical structures of both untreated and treated fiber were characterized by Fourier transform infrared spectroscopy. Results of mechanical test showed that the impact strength and elongation at break of PLA/Flax composites were remarkably higher than PLA. The impact fractures of PLA/Flax composites were also observed by scanning electron microscope. The results showed uniform dispersion of fibers in PLA matrix and good compatibility between treated fibers and PLA matrix. Moreover, it can be observed that crazing propagation was hindered by fibers and transcrystalline developed along fibers by polarized optical microscope. Differential scanning calorimetry analysis was carried out to study the crystallinity of PLA and it was found that incorporation of fiber improved the crystallinity of PLA. The toughening mechanism of PLA/Flax composites was discussed according to the results.

© 2015 Wiley Periodicals, Inc. *J. Appl. Polym. Sci.* **2015**, *132*, 42573.

**KEYWORDS:** biopolymers & renewable polymers; cellulose and other wood products; composites

Received 8 March 2015; accepted 1 June 2015

DOI: 10.1002/app.42573

### INTRODUCTION

Degradable polymers from renewable resources have been gradually gained ground over the last two decades because of energy and environment problems. Poly (lactic acid) (PLA) is one of the most potential candidates, not only because of its renewability, but also biodegradability and nontoxicity. PLA can be derived from renewable resources such as corn, sugar, cane, starch, etc. Besides, PLA has relatively high strength, high modulus, and adaptability to different processing techniques. Accordingly, it gained increasing interest over the past few decades. Nowadays, it is widely used in agriculture, medical applications and daily life, such as textiles, internal fracture fixation, plastic bags for household wastes, barriers for sanitary products and diapers, packaging of products, etc.

Like most polymers from petroleum, polymers from renewable resources are rarely used alone.<sup>1</sup> PLA has still not won any meaningful market acceptance as an engineering resin because of its nonsatisfying impact resistance.<sup>2</sup> In order to toughen and reinforce PLA, numerous approaches have been adopted such as block copolymerization, plasticization, blending with elastomers. One of the promising way was blending PLA with plant fiber such as hemp,<sup>3</sup> wood fibers,<sup>4</sup> bamboo cellulose fibers,<sup>5</sup> flax,<sup>6–8</sup> oil palm mesocarp fiber,<sup>9</sup> sisal,<sup>10</sup> jute<sup>11</sup> because of light weight, low density, low cost, high strength, high stiffness of plant fiber.

It does not mean that plant fiber always toughen and reinforce PLA. The degree of toughening is decided by many factors, such as, size, quantity, dispersion of fiber, processing conditions, etc. For instance, the PLA/coffee ground composites showed higher elongation than the PLA/bamboo flour composites because of the ether compounds in coffee ground according to Baek's investigation.<sup>12</sup> Composition, strength, and flexibility of fiber depend on categories, and contributions of different fibers to composites are different. Content of fiber is one of the hottest objects for researchers to explore PLA/plant fiber composites, composite with a suitable fiber content has optimum comprehensive mechanical properties. It is reported by Ho<sup>13</sup> that PLA/bamboo charcoal (BC) composite with 7.5 wt % BC exhibits the maximum impact strength. Furthermore, effect of preparation and processing on final performance of composites is profound. Song<sup>14</sup> blending-spun hemp and PLA fibers, heated and cut to obtain pellets. The pellets fed to extruder and injection molding machine to prepared PLA/hemp fiber composite. The impact strength of composite was improved nearly 68% compared with the neat PLA. In addition, additive can also influence toughness of composite. Intan<sup>15</sup> prepared PLA/kenaf composite containing up to 40% (w/w) of kenaf fiber, and revealed that the composites with 10% (w/w) thymol had higher flexibility compared with those systems containing lower concentrations of this additive. Wang<sup>16</sup> showed that the impact

© 2015 Wiley Periodicals, Inc.

**Table I.** Abbreviations of Fibers

Abbreviation	Surface modification
UF	Untreated flax fiber
AF	Alkali treated flax fiber
MF	Alkali-maleic anhydride treated flax fiber
KF	Alkali-silane KH550 treated flax fiber

strength of the PLA/bamboo fiber composite was improved with the use of PLA-g-GMA as the compatibilizer.

However, quite few studies focus on the reasons for toughening from many perspectives and reveal the toughening mechanism of PLA-based composites. In the present article, PLA/Flax composites with high toughness were fabricated via blending flax fiber with PLA to explore the toughening mechanism of PLA/Flax composites.

## EXPERIMENTAL

### Materials

PLA 6060D, extrusion grade, was supplied by Nature Works LLC., the melt point is 168°C. Flax fiber (the length is about 30–32 mm, and the average diameter is nearly 10–20 μm) was obtained from Zhengda chemical, China. The rest of reagents are of analytical grade, and used as received from Sinopharm Chemical Reagent.

### Fiber Surface Modifications

Flax fiber surfaces were modified by alkaline solution, maleic anhydride (MAH) and silane KH550. The fibers were labeled as shown in Table I. Raw flax fiber was incubated in sodium hydroxide (NaOH) solution for 7 h, followed by rinse and air-dried, denoted as AF, which was further treated with MAH, xylene, and dicumyl peroxide (DCP) in a flash at 110°C for 2 h, labeled as MF. The fiber was washed and dried, and MF samples were obtained. AF, silane KH550, ethanol, and deionized water in stoichiometric proportions were mixed and stand a while at 28°C, in which case KF was obtained.

### Fabrication of PLA/Flax Composites

Flax fiber and PLA were vacuum oven-dried prior to use at 107°C for 7 h and 60°C for 48 h, respectively. Dry PLA and fibers were introduced in twin-screw extruder (TE-34 type, Chemical Industry, Chemical Machinery Institute), the six zones temperatures of screw were 172°C, 175°C, 177°C, 177°C, 174°C, and 172°C, respectively, and the screw speed was 150 rpm. The quantity of fiber in composites was 5 wt %. The composites cords were pulled out from extruder, cooled in water bath, and were fed in granulator to be particles, vacuum oven-drying.

### Injection Moulding

Dry composite particles were fed to injection molding machine (HTF-80-W2 type, Ningbo Haitian, China) to prepare tensile, flexural, and impact test specimens. The four-section controlled temperature ranged from 177°C to 182°C; the injection pressure and the dwell pressure were set at 60 and 55 MPa, respectively; the mold temperature was controlled at 55 ± 1°C. The composites were summarized in Table II.

### Fibers, PLA, and PLA/Flax Composites Characterization

The functional groups of treated and untreated fibers were measured by a Nicolet 460 Fourier transform infrared spectroscopy (FTIR) spectrophotometer. Grounded dried fiber and potassium bromide (KBr) (2 mg fiber per 150 mg KBr) was pressed into a disc for FTIR measurement.

The tensile and bending strength, Young's modulus, and elongation at break were determined by computer-controlled electronic universal testing machine CMT-5104 (Sans Measuring Technology, Shenzhen of China) with a loading cell of 10 kN. Tensile test followed ASTM-D683 standard, and dimensions of tensile specimen belonged to type I of ASTM-D683 standard. Initial grip separation of tensile test was set at 50 mm, and stretching speed was at 5 mm/min; Initial grip separation of bending test was set at 70 mm, press speed was at 2 mm/min. The Izod impact strength was tested by a cantilever beam impact tester (XCJ type, Science and Education Instrument Plant of Jilin University, China). The specimens were non-notched, and dimension of specimens is 63.5 mm × 10.0 mm × 4.0 mm. All mechanical tests took place at 40% relative humidity and 21°C. The specimens had been conditioned under the same circumstances for 7 days before testing. The data were averaged from measurements of five specimens.

The impact fracture sections of PLA and PLA/Flax composites were observed by scanning electron microscope (SEM) (AUANTA 200 type, JEOL., Japan), operated at 20 kV. Before SEM observation, a Pt layer of 20–30 nm was coated on the impact fracture surfaces.

Crystalline structures of PLA and PLA/KF were seen from polarized optical microscope (POM) (59XC type, Shanghai instrument factory six, China). Before insulation at 152–155°C for 30 min, the whole samples thoroughly melt at 175–180°C.

The melting and crystallization behavior of neat PLA and PLA/Flax composites were investigated on Differential scanning calorimetry (DSC) 6 Perkin Elmer instrument with sample weight of about 10 mg. The sample was heated from 50°C to 200°C at a rate of 10°C/min under nitrogen atmosphere. The crystallinity (%) of the PLA was calculated from the following equation<sup>17</sup>:

$$\% \text{ Crystallinity} = (\Delta H_m / w \times \Delta H_0) \times 100\% \quad (1)$$

where  $\Delta H_m$  is heat of melting of sample,  $\Delta H_0$  is heat of melting of 100% crystalline PLA i.e., 93 J/g,<sup>18</sup> and  $w$  is the mass fraction of PLA in composite.

**Table II.** Abbreviations of Composites

Number	Sample
PLA	Neat PLA
PLA/UF	PLA/untreated fiber composite
PLA/AF	PLA/alkali-treated fiber composite
PLA/MF	PLA/alkali-maleic anhydride-treated fiber composite
PLA/KF	PLA/alkali-silane KH550-treated flax fiber composite

**Table III.** Mechanical Properties of Neat PLA and PLA/Flax Composites

Number	Tensile strength (MPa)	Bending strength (MPa)	Tensile modulus (GPa)	Bending modulus (GPa)	Elongation at break (%)	Impact strength (kJ/m <sup>2</sup> )
PLA	54.1 ± 0.4	91.9 ± 4.4	2.68 ± 0.04	3.7 ± 0.1	2.62 ± 0.08	13.3 ± 0.5
PLA/UF	59.5 ± 1.7	90.2 ± 6.0	3.38 ± 0.16	3.9 ± 0.4	6.06 ± 0.43	14.8 ± 0.5
PLA/AF	58.4 ± 2.0	91.7 ± 2.9	3.26 ± 0.12	4.1 ± 0.1	7.05 ± 0.22	15.1 ± 0.1
PLA/MF	57.6 ± 0.6	92.8 ± 1.9	2.78 ± 0.10	4.1 ± 0.1	7.98 ± 0.33	14.4 ± 0.6
PLA/KF	58.1 ± 0.8	91.9 ± 0.3	3.00 ± 0.09	3.9 ± 0.1	9.76 ± 0.62	16.1 ± 0.1

Neat PLA pellets were dissolved in chloroform to obtain solution, and PLA/KF composite was dissolved in chloroform to obtain suspension. The concentration of solution and suspension was controlled at 50 mg/mL. The solution and suspension were dropped onto micro-slide, dried at 20°C for 48 h. The thickness of PLA and PLA/Flax composites films was 0.10 mm. Films were stretched by electronic universal testing machine CMT-5104. Initial grip separation of tensile test was set at 20 mm, and stretching speed was at 10 mm/min. The tensile tests were stopped when films yielded, and the stretched films were observed by optical microscope.

## RESULTS AND DISCUSSION

### Mechanical Properties of PLA and PLA/Flax Composites

Table III shows mechanical properties of neat PLA and PLA/Flax composites. The tensile strength of PLA/Flax composites was slightly higher than that of PLA, while bending strength of PLA and PLA/Flax composites was similar, nearly 91 MPa. In Sunil's research,<sup>19</sup> the tensile strength of virgin PLA reduced by the introduction of banana fiber because of the nonuniform stress transfer from matrix to fibers. Many other studies<sup>20,21</sup> also found that the tensile and flexural strength of the composites became poorer as the introduction of natural vegetable fiber.

By contrast, Young's Modulus of PLA/Flax composites was higher than that of neat PLA. The increase of modulus agrees with other works<sup>22,23</sup> proposed by previous researchers. Studies suggested that Young's modulus of composites increased because of the high Young's modulus character of nature fiber.

Table III shows the elongation at break and impact strength of PLA and PLA/Flax composites. Elongation at break and impact strength of PLA were 2.62 ± 0.08% and 13.3 ± 0.5 kJ/m<sup>2</sup>, respectively, implying that PLA was very brittle. The ductility and toughness dramatically increased by incorporation of fiber, elongation at break, and impact strength of composites were higher than neat PLA. Furthermore, the and toughness of PLA/KF was the best among the composites because of strong interaction between KF and PLA, elongation at break, and impact strength improved about 270% and 20% compared with neat PLA, respectively.

The bending strength of composites was similar to that of PLA, while the tensile strength, Young's modulus, elongation at break, and impact strength of composites were higher than PLA, which indicates that the addition of flax fiber improves the mechanical properties of materials. Surface modifications of fiber lead to

increase of the elongation at break and impact strength, yielding PLA/KF of best performance in toughness.

The stress–strain curves of PLA and PLA/Flax composites were collected during the tensile test as shown in Figure 1. At initial stage, strain increased with increasing stress, which belongs to the Hooker elastic deformation. With the continued increasing of stress, crazing appeared in PLA and PLA/Flax composites. Crazing is an important deformation mechanism observed in amorphous polymers, which can absorb energy.<sup>24</sup> For PLA, samples ruptured with very low elongation, this is typical brittle fracture as shown with solid line in Figure 1.

Comparing curves of PLA/Flax composites with PLA, it was easy to find that fracture behavior of the PLA/Flax composites was different from PLA. After linear deformation and yielding, crazing emerged continuously, and PLA molecular chain stretched and oriented under external force, which provided condition for large-deformation. Accordingly, stress was almost unchanged, while strain increased significantly in the stress-strain curves. This region was called the strain-hardening region.<sup>25</sup> More crazing and macromolecular chain orientation

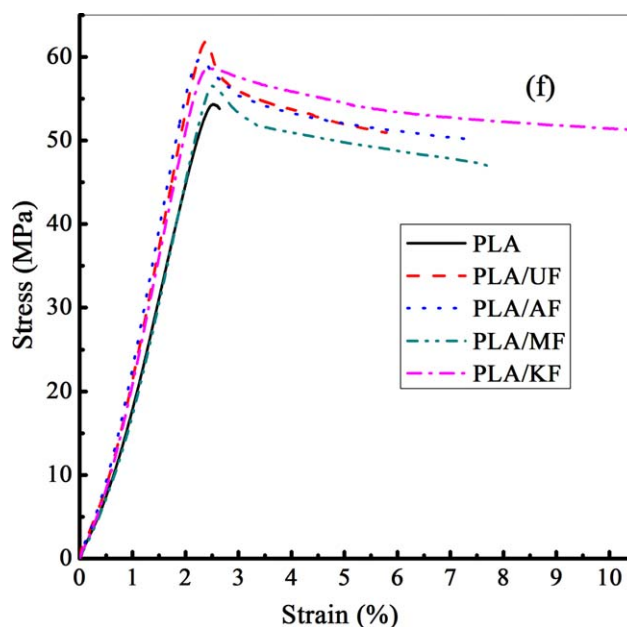


**Figure 1.** Comparative plot of tensile stress–strain curves of PLA and PLA/Flax composites. [Color figure can be viewed in the online issue, which is available at [wileyonlinelibrary.com](http://wileyonlinelibrary.com).]

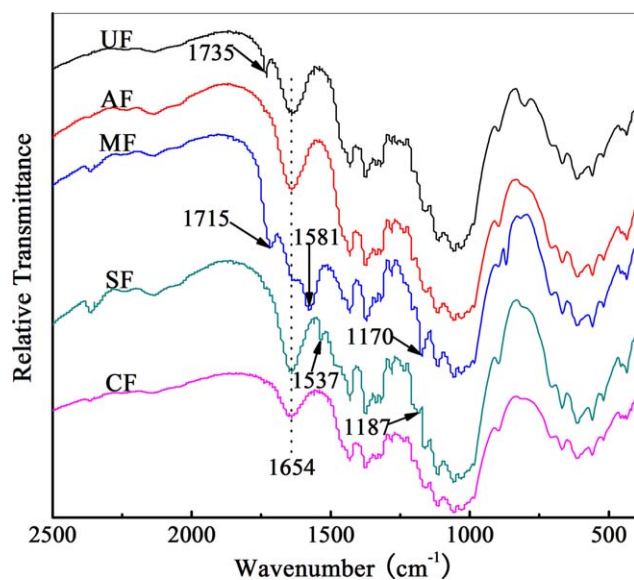


**Figure 2.** FTIR Spectra of treated and untreated flax fibers. [Color figure can be viewed in the online issue, which is available at [wileyonlinelibrary.com](http://wileyonlinelibrary.com).]

tended to result in higher strain-at-break. Fracture behavior of the PLA/Flax composites belonged to typical ductile fracture. However, the result was opposite in other researches, elongation at break and toughness of polymer/nature composites were smaller and poorer than that of pure polymer because of poor compatibility or dispersibility.<sup>26–28</sup>

Furthermore, it can be seen from Figure 1, tensile strength, tensile modulus, and elongation at break of PLA/Flax composites were higher than PLA, and surface modifications of fiber increased the elongation at break of composite markedly.

#### Reasons for Flax Fiber Toughening PLA

Flax fibers were able to toughen PLA obtaining high toughness composites, which may attribute to the following four factors: (1) good compatibility between fibers and matrix; (2) uniform distribution of fibers in the matrix; (3) the structure of flax fibers; and (4) crystalline improvement. Next, the four factors will be demonstrated and explored in depth.

**Good Compatibility between Fiber and Matrix.** Figure 2 shows FTIR spectra of untreated and treated flax fibers, the peak at  $1735\text{ cm}^{-1}$  was considered because of the absorption of carbonyl (C=O) stretching of hemicelluloses, pectin,<sup>29</sup> and lignin present in UF. The peak at  $1735\text{ cm}^{-1}$  disappeared in AF, MF, and KF samples. It might be because of the removal of hemicelluloses, pectin, and lignin present in the fibers<sup>30</sup> by alkali treatment. No absorption in the region of around  $1780\text{--}1850\text{ cm}^{-1}$  in MF indicated that there was no residual MAH. The peak of C=O group at  $1715\text{ cm}^{-1}$  and the peak of CH=CH at  $1581\text{ cm}^{-1}$  appeared, and the peak of C—O at  $1170\text{ cm}^{-1}$  became strong in MF, which provided evidence of existence of —OCO—CH=CH—COOH and successful maleation in MF. A new peak at  $1537\text{ cm}^{-1}$  was attributed to the N—H, and the characteristic band at  $1187\text{ cm}^{-1}$  corresponds to asymmetric Si—O—C stretching in KF, which confirmed the successful sili-

nization of KF.<sup>31</sup> Alkali treatment<sup>32,33</sup> maleation<sup>34</sup> and silanization<sup>35</sup> of fiber can improve the compatibility between fiber and polymer matrix.

The influences of filler surface treatment on the mechanical properties and impact fractured surfaces morphology were frequently observed.<sup>36,37</sup> Figure 3 shows the SEM images of impact surface panorama of PLA and PLA/Flax composites. The fracture section of PLA was relatively flat and smooth<sup>38</sup> as shown in Figure 3(a), indicating brittle rupture. The fracture surface of PLA/UF was presented in Figure 3(b), was obvious coarser than neat PLA, indicating that UF toughened PLA to some extent. However, the compatibility between fibers and matrix was poor because of the inherently hydrophilic character of raw flax fibers and hydrophobic feature of PLA, which resulted in poor toughness behavior of PLA/UF. By contrast, impact fracture surfaces of PLA/AF, PLA/MF and PLA/KF were rougher than PLA/UF, implying compatibility of fibers and matrix was improved. Plastic deformation scattered in the wide area without interfacial failure, leading to rough fracture surfaces.

In summary, good interface compatibility allows a greater force transfer from the matrix to the fibers,<sup>39</sup> which is one of causes for flax fiber toughening PLA.

**Uniform Distribution of Fiber in the Matrix.** Fiber dispersion plays a critical role in controlling various properties of polymer composites.<sup>40</sup> However, Aggregation usually happened because of the entanglement and low apparent density of fiber. Fiber dispersion in matrix can be observed from Figure 3(b–e). Aggregation or entanglement was not noticed in these pictures, meanwhile fibers sporadically and randomly scattered in/on the impact fracture surfaces. PLA/Flax composites fabricated by extrusion and injection molding, two melt-based processes accelerated separation of fibers in the composites and prohibited fibers from aggregating. Moreover, low fiber loading (5 w %) maybe the other reason why there were no aggregations. This result was beneficial to guarantee uniform stress transfer from matrix to fibers and homogeneous properties of composites, which was optimal for toughening to occur.<sup>41</sup>

**The Structure of Flax Fiber.** Single flax fiber consists of numerous microfibrils, these microfibrils stack neatly and orientate along axial direction. The Van der Waals force and hydrogen bond bind the microfibrils side-by-side together. The microfibrils are formed by cellulose molecules crystallizing and orienting. The special chemical and physical structures make flax fiber have super flexible feature. As filler, flax fiber is usually used to toughen and reinforce polymer materials.

Figure 4 is showing impact fracture surface details of PLA and PLA/Flax composites, as well as fracture patterns of fiber. The fracture section of PLA was more flat and smooth than PLA/KF. The formations of fiber fracture included pulling out, tearing into microfibrils and pulling-tearing combination, and fiber fracture formations were decided by the included angle between fiber axial direction and impact force direction. Fibers were pulled out from matrix, leaving small holes on one side and fiber stubbles on the other side, when the included angle



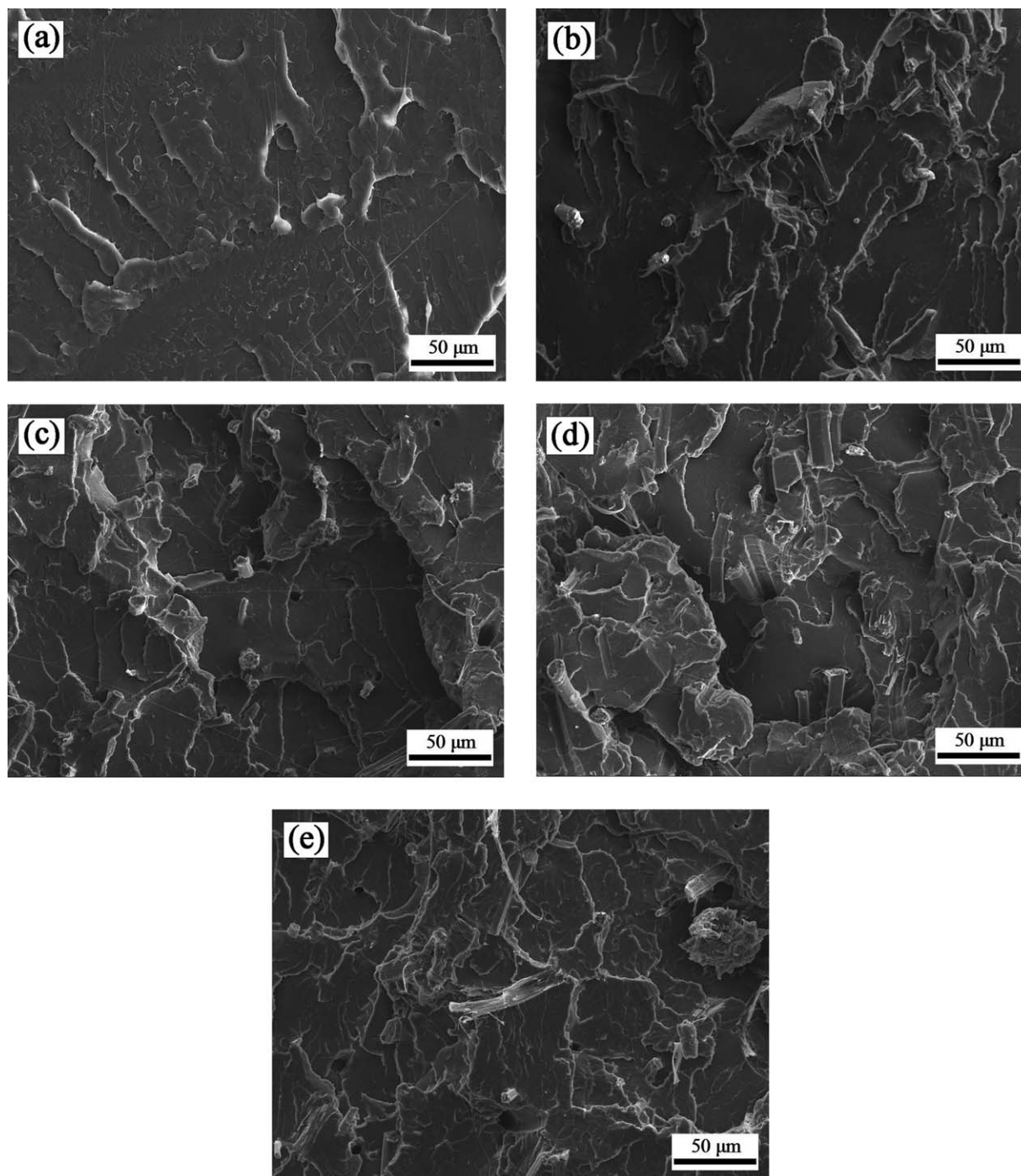


**Figure 3.** SEM images of impact surface panorama of (a) PLA, and (b) PLA/UF, (c) PLA/AF, (d) PLA/MF, (e) PLA/KE.

was  $90^\circ$ . The holes and stubbles were visible in/on the fracture surfaces, and axial direction of stubble was perpendicular to fracture surface as shown in Figure 4(b). Fibers were tore into microfibers when the included angle was  $0^\circ$  as shown in Figure 4(c). Crack propagated along fiber axial direction, and intruded into fiber bundle, which caused that fiber bundle was transversely cleaved. Residual fiber bundle lay flat in/on the fracture surface. Pulling-tearing combination was another fracture method of fiber under large impact, which is shown in Figure 4(d). Both microfibers and stubbles can be seen in the

same fiber, stubbles attribute to pulling out of fibers, and microfibers resulted from split of fiber bundles. The included angle between stubble and fracture surface is a certain angle ( $0-90^\circ$ ). Fibers fracture absorbed large energy and upgraded the impact strength by pulling out, tearing into microfibers and pulling-tearing combination.

Flax fibers are able to toughen polymer not only because fibers fracture absorbed large energy, but also because fibers can hinder and weaken propagation of crazing and cracks to some extent.

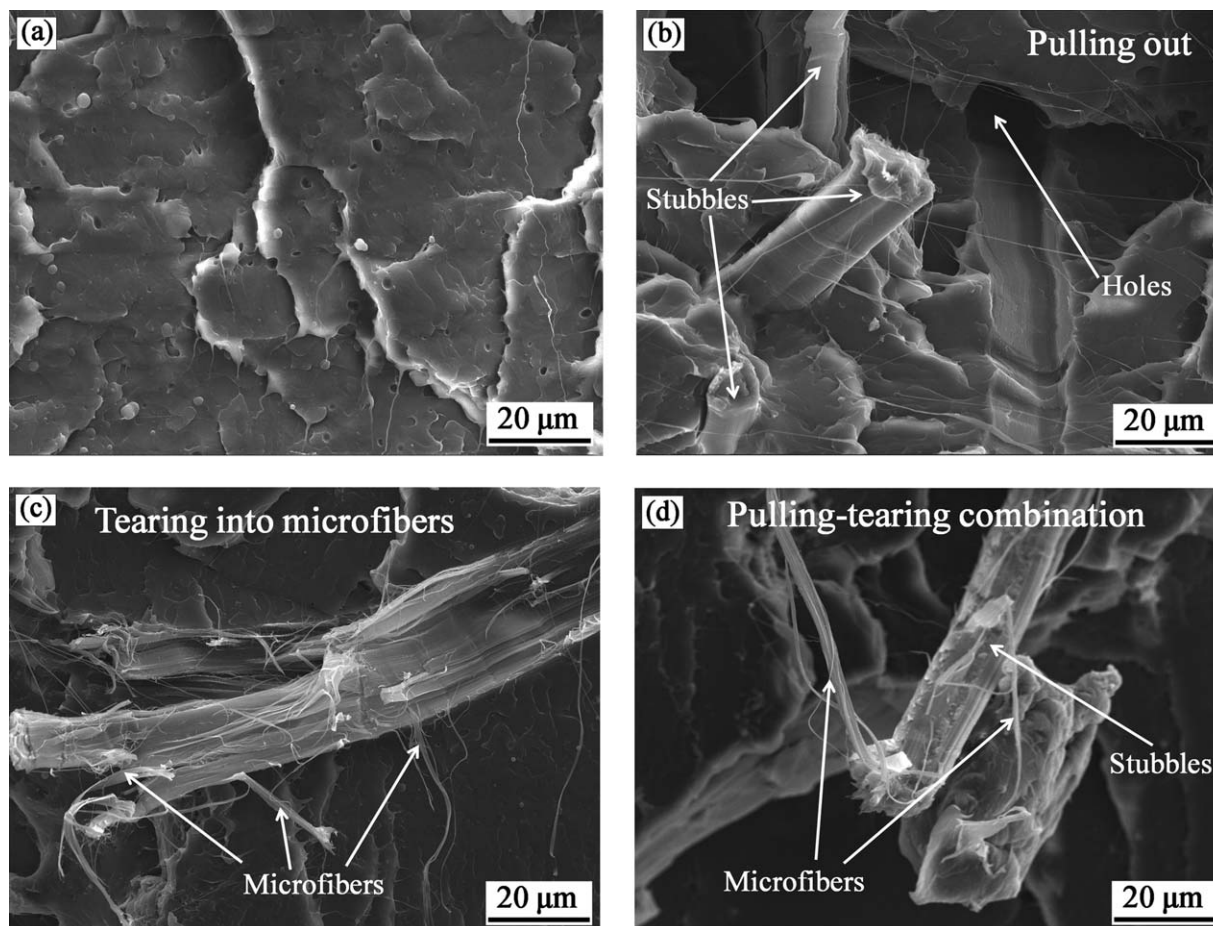


Figure 4. SEM images of impact fracture surface details of (a) PLA and (b,c,d) PLA/KF.

Optical micrographs of stretched films of PLA and PLA/KF are shown in Figure 5. Cracking generated under large stress, and propagated ahead with increasing of stress. Cracking of PLA propagated successfully without facing obstacles, and the operation was like splitting the bamboo, as shown in Figure 5(a,b). On the contrary, the situation of PLA/KF was different. Abundant of cracking came across fibers when propagated forward, and was hindered by fibers. A new little part of cracking generated on the other side of fiber with increasing of stress, propagated forward, and faced new fibers again. Cracking decreased and weakened along the orientation of propagating as shown in Figure 5(c,d) with arrows. Of course, fibers might be destroyed under large stress. Strength and toughness of material would be improved to some extent when cracking was hindered and weakened.

**Changed of the Crystalline.** Crystalline morphologies and sizes have effects on toughness of materials. The crystal photos of PLA and PLA/KF are shown in Figure 6. It is easy to find that PLA and PLA/Flax composites could complete crystallization. It is very interesting to observe that the crystal grew along flax fibers in composites, and crystal preferred to nucleate at node sites [see Figure 6(b)] and end of fibers [as marked in Figure 6(c,d)]. The PLA molecules were nucleated on the flax fiber surface, and transcrystallization grew along fibers. On one hand,

compact transcrystallization structure was beneficial for hindering and weakening cracking propagation. Furthermore, transcrystallization improved adhesion strength between the fibers and matrix.<sup>42</sup> In summary, transcrystallization had positive influences on toughening PLA.

In addition, large spherulite size of neat PLA was approximately 200  $\mu\text{m}$ , while size of transcrystallization was nearly 100  $\mu\text{m}$  at most. The diminution of crystal size is good for toughness. It is generally agreed that impact resistance is inversely related to spherulite size.<sup>43</sup> Ohlberg *et al.*<sup>44</sup> found that impact strength decreased with spherulite size increasing when crystallization in high-density poly(ethylene) was studied. Hammer *et al.*<sup>45</sup> studied crystallization in poly(propylene), and found that samples with larger spherulites lost ductility. Wright *et al.*<sup>46</sup> noted that impact strength decreased with increasing spherulite size. Spherulite size increased, and the interlamellar and interspherulitic connections became weaker, which was favorable to fracture during tension and so a small elongation at break was obtained.<sup>47</sup>

DSC analysis was carried out to study the melting and crystallization behavior of PLA after addition of UF, AF, MF, and KF, results are shown in Figure 7 and Table IV. Cold crystallization and melt behaviors of PLA and PLA/Flax composites could be seen From Figure 7. The maximum improvements in cold



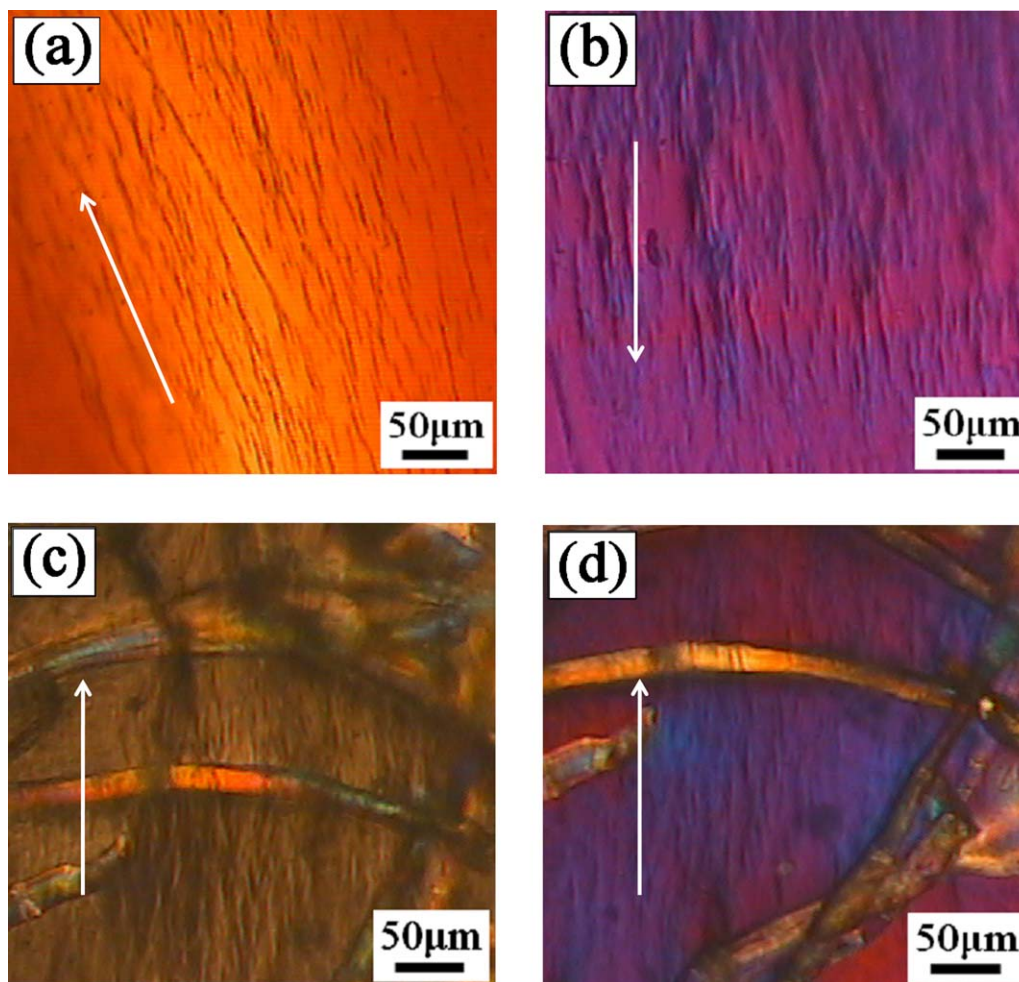


**Figure 5.** Optical micrographs of stretched (a,b) PLA, and (c,d) PLA/KF films; (a) and (c) were observed with natural light, (b) and (d) were observed with polarized light; arrows show the direction of crazing propagation. [Color figure can be viewed in the online issue, which is available at wileyonlinelibrary.com.]

crystallization temperature ( $T_{cc}$ ) value was observed for PLA/UF composites where  $T_{cc}$  was increased from 105.8°C to 109°C. The increase in  $T_{cc}$  could be attributed to the existence of UF. UF hindered mobility of PLA chains, led to lack of chain flexibility. In addition, it was difficult for PLA chains to get attached UF surface to perform cold crystallization because of weak interaction between PLA matrix and UF. Table IV indicates that melting temperature ( $T_m$ ) of neat PLA and PLA/Flax composites do not change significantly with incorporation and surface modification of fiber. The addition of fiber in PLA matrix found to improve the crystallinity of PLA, and surface treatments improved the crystallinity of PLA ulteriorly as shown in Table IV.

#### Toughening Mechanism of PLA/Flax Composites

Toughening mechanism schematic diagram of PLA/Flax composites is shown in Figure 8. Neat PLA was subjected to large impact during impact test, cracks generated inexorably in a short moment, and grew very fast under irresistible force. Cracks highly would cause fatal deterioration at early stage, the whole sample broke suddenly without any obstructions. So, the

fracture surfaces were smooth and tidy [see Figures 3(a) and 4(a)].

For PLA/Flax composites, as previously described and seen, fibers distributed in PLA matrix randomly, implying that the included angle between impact force and axial direction of fiber may range from 0° to 90°. Under large impact force of pendulum bob, cracks inexorably occurred in PLA/Flax composite, and came across fibers on its way to propagation. When the included angle is 90° [see Figure 8(b)], namely, axial direction of fiber is perpendicular to the direction of force, the cracks cannot propagate straightly and favorably on account of fibers and interfacial transcrystallization [shown in Figure 6(b–d)]. This transcrystallization was as firm as rampart to resist cracks. Cracks could not arrive at fiber surface until transcrystallization was destroyed. It was hard for crack tip to penetrate into the interior of fiber bundle, unless the orientational microfibers are cut down. Before that, crack tips became more obtuse in front of fiber. The impact dynamics dispersed to wider area than ago, the impact was diluted, weakened, and intensity of force on the unit area decreased. Flax fibers and transcrystallization can assist in dissipating or absorbing the energy.<sup>48</sup> At last, microfibers

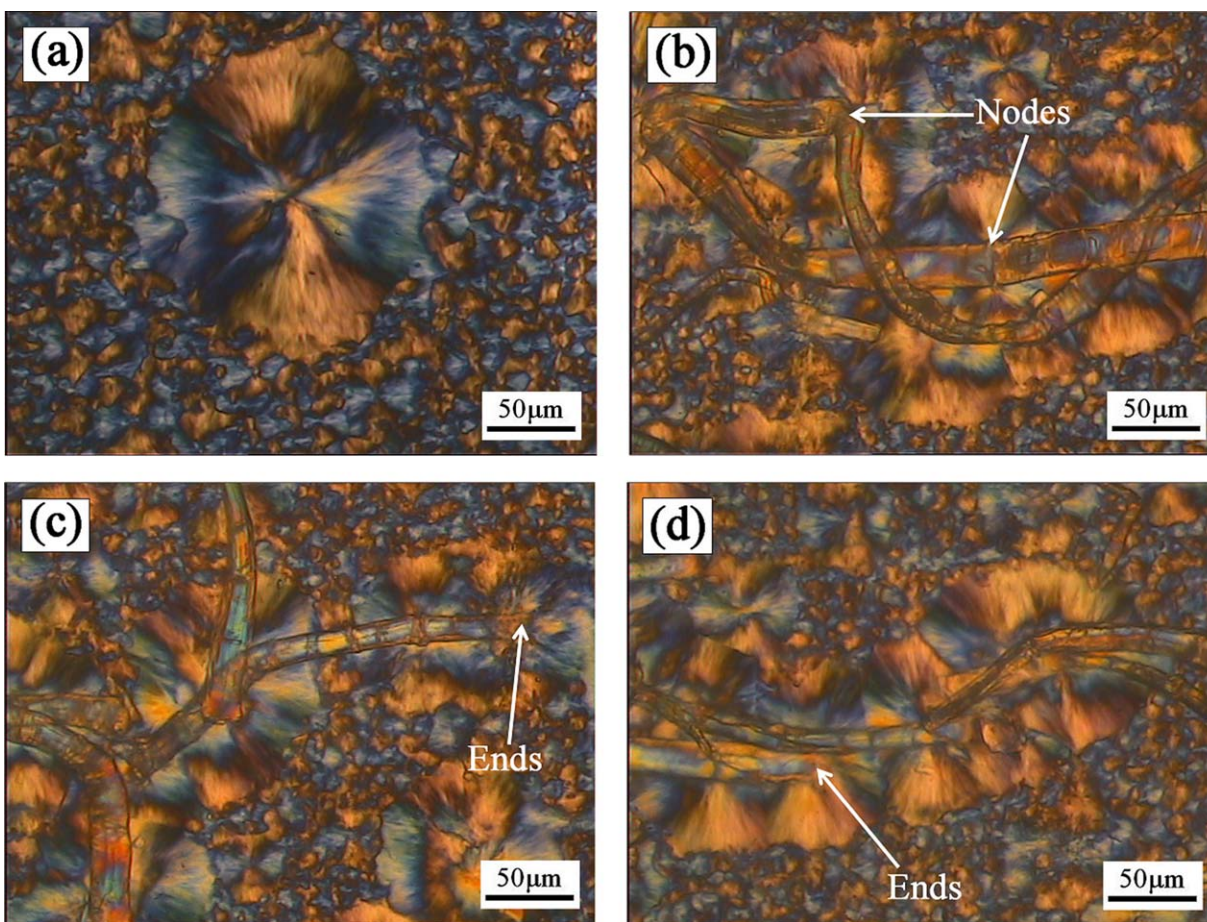


**Figure 6.** Crystal photos of (a) PLA and (b,c,d) PLA/KF. [Color figure can be viewed in the online issue, which is available at [wileyonlinelibrary.com](http://wileyonlinelibrary.com).]

were cut, following fiber bundles were pulled out leaving holes on one side and stubble on the other side of fracture surface [see Figure 4(b)]. In sum, destroying transcrystallization, cutting fiber bundles would absorb energy; impact dynamics dispersion

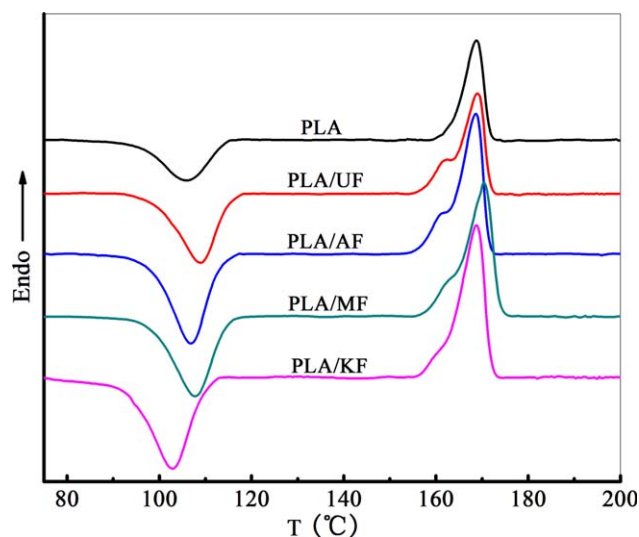


**Figure 7.** DSC of neat PLA and PLA/Flax composites. [Color figure can be viewed in the online issue, which is available at [wileyonlinelibrary.com](http://wileyonlinelibrary.com).]

made it more difficult to break sample, which improved the toughness of composites.

When the included angle is  $0^\circ$ , the crack caused by impact may encounter fiber end, as can be seen from Figure 8(c). To intrude into fiber, the crack must break the PLA spherocrystal of fiber end at first [see Figure 6(c, d)]. Once the crack tip squeezed into fiber, Cellulose microfibril bundles were transversely cleaved, which could be seen in Figure 4(c). In summary, destroying spherocrystal and fiber bundle being split into microfibrils would absorb energy, which could upgrade the toughness of composites.

Actually, the condition of  $90^\circ$  and  $0^\circ$  are rare, for the most conditions, the included angle is a certain angle between  $0^\circ$  and  $90^\circ$  as shown in Figure 8(d). Flax fibers absorbed impact energy by pulling-tearing comprehensive pattern [see Figures 4(d) and 8(d)], improving toughness of PLA/Flax composites. Destroying transcrystallization, hindering and weakening propagation of cracks, absorbing impact energy by pulling-tearing fiber improved the toughness of PLA/Flax composites.

## CONCLUSIONS

1. Treated flax fibers were blended with PLA by melt extrusion and injection moulding to prepare PLA/Flax composites.



**Table IV.** Crystallization and Melting Behavior of PLA and PLA/Flax Composites

Number	$T_{cc}$ (°C)	$T_m$ (°C)	$\Delta H_m$ (J/g)	Crystallinity (%)
Neat PLA	105.8	168.7	17.4	18.7
PLA/UF	109.0	169.0	22.8	21.2
PLA/AF	106.8	168.6	26.8	30.3
PLA/MF	107.8	170.4	26.1	29.5
PLA/KF	102.9	168.8	25.9	29.3

The tensile strength, Young's modulus, elongation at break, and impact strength of PLA/Flax composites were higher than that of neat PLA. Fiber surface modification improved toughness of composites, and elongation at break and impact strength of PLA/KF increased up to 270% and 20% comparing with PLA, respectively.

- Good compatibility between fibers and matrix, uniform distribution of fibers in the matrix, cracks propagation being hindered by fibers, energy being absorbed with fiber fracture and transcrystallization were mainly reasons for toughening.
- Fibers toughen PLA by three modes, which are decided by the included angle between impact force and axial direction

of fiber. Firstly, fiber is pulled out when the included angle is 90°. Secondly, fiber bundle being tore into microfibrils would absorb energy when the included angle is 0°. The last, the fibers are broken by a pull-out and tear-into-microfiber comprehensive formation when the included angle is between 90° and 0°.

#### ACKNOWLEDGMENTS

This work reveals flax fibers toughening PLA by hindering propagation of cracks, absorbing energy with pulling out fiber and tearing into microfibrils.

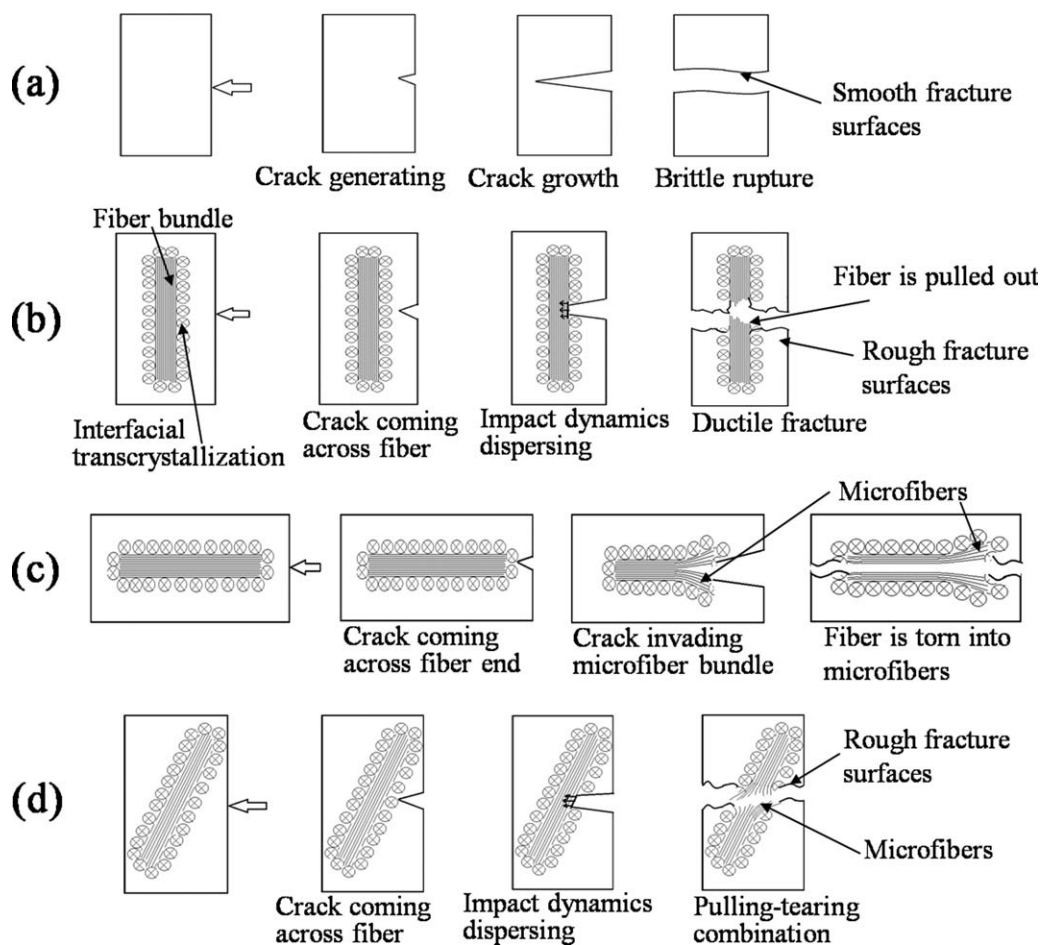


**Figure 8.** Toughening mechanism schematic diagram of PLA/Flax composites, (a) PLA, the included angles between impact force and axial direction of fiber were (b) 90°, (c) 0°, (d) 0–90°.

## REFERENCES

1. Yu, L.; Dean, K.; Li, L. *Prog. Polym. Sci.* **2006**, *31*, 576.
2. Bledzki, A. K.; Jazzkiewicz, A.; Scherzer, D. *Compos. A.* **2009**, *40*, 404.
3. Baghaei, B.; Skrifvars, M.; Berglin, L. *Compos. A* **2013**, *50*, 93.
4. Awal, A.; Rana, M.; Sain, M. *Mech. Mater.* **2015**, *80*, 87.
5. Lu, T.; Liu, S.; Jiang, M.; Xu, X.; Wang, Yong.; Wang, Z.; Gou, Jan.; Hui, D.; Zhou, Z. *Compos. B* **2014**, *62*, 191.
6. Linganiso, L. Z.; Bezerra, R.; Bhat, S.; John, M.; Braeuning, R.; Anandjiwala, R. D. *J. Thermoplast. Compos.* **2014**, *27*, 1553.
7. Alimuzzaman, S.; Gong, R. H.; Akonda, M. *Polym. Compos.* **2014**, *35*, 1244.
8. Alimuzzaman, S.; Gong, R. H.; Akonda, M. *Polym. Compos.* **2014**, *35*, 2094.
9. Eng, C. C.; Ibrahim, N. A.; Zainuddin, N.; Ariffin, H.; Wan, Z. W. Y. *Sci. World J.* **2014**, *2014*, 1.
10. Orue, A.; Jauregi, A.; Rodriguez, C. P.; Labidi, J.; Eceiza, A.; Arbelaiz, A. *Compos. A* **2015**, *73*, 132.
11. Arao, Y.; Fujiura, T.; Itani, S.; Tanaka, T. *Compos. B* **2015**, *68*, 200.
12. Baek, B. S.; Park, J. W.; Lee, B. H.; Kim, H. J. *J. Polym. Environ.* **2013**, *21*, 702.
13. Ho, M. P.; Lau, K. T. *Mater. Lett.* **2014**, *136*, 122.
14. Song, Y.; Liu, J.; Chen, S.; Zheng, Y.; Ruan, S.; Bin, Y. *J. Polym. Environ.* **2013**, *21*, 1117.
15. Tawakkal, I. S. M. A.; Cran, M. J.; Bigger, S. W. *Ind. Crop. Prod.* **2014**, *61*, 74.
16. Wang, Y. N.; Weng, Y. X.; Wang, L. *Polym. Test.* **2014**, *36*, 119.
17. Fisher, E. W.; Sterzel, H. J.; Wegner, G. *Colloid. Polym. Sci.* **1973**, *251*, 980.
18. Baheti, V.; Militky, J.; Marsalkova, M. *Polym. Compos.* **2013**, *34*, 2133.
19. Majhi, S. K.; Nayak, S. K.; Mohanty, S.; Unnikrishnan, L. *Int. J. Plast. Technol.* **2010**, *14*, 57.
20. Li, S.; Wang, C.; Zhuang, X.; Hu, Y.; Chu, F. *J. Polym. Environ.* **2011**, *19*, 301.
21. Sayeed, M. M. A.; Rawal, A.; Onal, L.; Karaduman, Y. *Polym. Compos.* **2014**, *35*, 1044.
22. Bax, B.; Müssig, J. *Compos. Sci. Technol.* **2008**, *68*, 1601.
23. Raj, G.; Balnois, E.; Baley, C.; Grohens, Y. *Int. J. Polym. Sci.* **2011**, *2011*, 1.
24. Hughes, J.; Thomas, R.; Byun, Y.; Whiteside, S. *Carbohydr. Polym.* **2012**, *88*, 165.
25. Ho, M.; Wang, H.; Lau, K. *Appl. Surf. Sci.* **2012**, *258*, 3948.
26. Suryanegara, L.; Nakagaito, A. N.; Yano, H. *Compos. Sci. Technol.* **2009**, *69*, 1187.
27. Bledzki, A. K.; Jazzkiewicz, A. *Compos. Sci. Technol.* **2010**, *70*, 1687.
28. Pracella, M.; Chionna, D.; Anguillesi, I.; Kulinski, Z.; Piorkowska, E. *Compos. Sci. Technol.* **2006**, *66*, 2218.
29. Sawpan, M. A.; Pickering, K. L.; Fernyhough, A. *Compos. A.* **2011**, *42*, 888.
30. Ouajai, S.; Shanks, R. A. *Polym. Degrad. Stab.* **2005**, *89*, 327.
31. Moigne, N. L.; Longerey, M.; Taulemesse, J. M.; Bénézet, J. C.; Bergeret, A. *Ind. Crop Prod.* **2014**, *52*, 481.
32. Fiore, V.; Bella, G. D.; Valenza, A. *Compos. B* **2015**, *68*, 14.
33. Sundaram, S. K.; Jayabal, S. *J. Polym. Eng.* **2014**, *34*, 839.
34. Reza, E. F. *Adv. Compos. Mater.* **2015**, *24*, 27.
35. Ifuku, S.; Yano, H. *Int. J. Biol. Macromol.* **2015**, *74*, 428.
36. Xue, Y.; Veazie, D. R.; Glinsey, C.; Horstemeyer, M. F.; Rowell, R. M. *Compos. B* **2007**, *38*, 152.
37. Pracella, M.; Haque, M. M. U.; Alvarez, V. *Polymer* **2010**, *2*, 554.
38. Jonoobi, M.; Harun, J.; Mathew, A. P.; Oksman, K. *Compos. Sci. Technol.* **2010**, *70*, 1742.
39. Yu, T.; Li, Y.; Ren, J. *Nonferrous Met. Soc. Chn.* **2009**, *19*, 651.
40. Li, Z.; Gao, Y.; Moon, K. S.; Yao, Y.; Tannenbaum, A.; Wong, C. P. *Polymer* **2012**, *53*, 1571.
41. Huda, M. S.; Drzal, L. T.; Misra, M. *Ind. Eng. Chem. Res.* **2005**, *44*, 5593.
42. Masirek, R.; Kulinski, Z.; Chionna, D.; Piorkowska, E.; Pracella, M. *J. Appl. Polym. Sci.* **2007**, *105*, 255.
43. Perkins, W. G. *Polym. Eng. Sci.* **1999**, *39*, 2445.
44. Ohlberg, S. M.; Roth, J.; Raff, R. A. V. *J. Appl. Polym. Sci.* **1959**, *1*, 114.
45. Hammer, C. F.; Koch, T. A.; Whitney, J. F. *J. Appl. Polym. Sci.* **1959**, *1*, 169.
46. Wright, D. G. M.; Dunk, R.; Bouvart, D.; Autran, M. *Polymer* **1988**, *29*, 769.
47. Han, L.; Han, C.; Dong, L. *Polym. Int.* **2013**, *62*, 295.
48. Petinakis, E.; Yu, L.; Edward, G.; Dean, K.; Liu, H.; Scully, A. D. *J. Polym. Environ.* **2009**, *17*, 83.